



This open access document is posted as a preprint in the Beilstein Archives at <https://doi.org/10.3762/bxiv.2022.66.v1> and is considered to be an early communication for feedback before peer review. Before citing this document, please check if a final, peer-reviewed version has been published.

This document is not formatted, has not undergone copyediting or typesetting, and may contain errors, unsubstantiated scientific claims or preliminary data.

Preprint Title Endocytosis and transport of silica nanoparticles in BeWo b30 cells

Authors Hongbo Tang, Weijie Jiang, Xin Feng, Yetao Chen, Junyu He, Mengyao Wu, Chenghong Yin and Haibo He

Publication Date 08 Aug 2022

Article Type Full Research Paper

ORCID® iDs Hongbo Tang - <https://orcid.org/0000-0003-3048-8353>

Title:

Endocytosis and transport of silica nanoparticles in BeWo b30 cells

The full names, institutional affiliations and emails of the authors:

- 1) Hongbo Tang, Department of Pharmacy, Beijing Obstetrics and Gynecology Hospital, Capital Medical University. Beijing Maternal and Child Health Care Hospital. Beijing, 100026, People's Republic of China.
Email: tanghongbo@ccmu.edu.cn
- 2) Weijie Jiang, Hubei Key Laboratory of Natural Products Research and Development, College of Biological and Pharmaceutical Sciences, China Three Gorges University, Yichang, Hubei, 443002, People's Republic of China.
Email: 1528591912@qq.com
- 3) Xin Feng, Department of Pharmacy, Beijing Obstetrics and Gynecology Hospital, Capital Medical University. Beijing Maternal and Child Health Care Hospital. Beijing, 100026, People's Republic of China.
Email: fengxin1115@ccmu.edu.cn
- 4) Yetao Chen, Hubei Key Laboratory of Natural Products Research and Development, College of Biological and Pharmaceutical Sciences, China Three Gorges University, Yichang, Hubei, 443002, People's Republic of China.
Email: 530896551@qq.com
- 5) Junyu He, Hubei Key Laboratory of Natural Products Research and Development, College of Biological and Pharmaceutical Sciences, China Three Gorges University, Yichang, Hubei, 443002, People's Republic of China.
Email: 3118242774@qq.com
- 6) Mengyao Wu, Hubei Key Laboratory of Natural Products Research and Development, College of Biological and Pharmaceutical Sciences, China Three Gorges University, Yichang, Hubei, 443002, People's Republic of China.
Email: 1441760315@qq.com
- 7) Chenghong Yin (Corresponding author), Department of Pharmacy, Beijing Obstetrics and Gynecology Hospital, Capital Medical University. Beijing Maternal and Child Health Care Hospital. Beijing, 100026, People's Republic of China. Email: yinchh@ccmu.edu.cn
- 8) Haibo He (Corresponding author), Hubei Key Laboratory of Natural Products Research and Development, College of Biological and Pharmaceutical Sciences, China Three Gorges University, Yichang, Hubei, 443002, People's Republic of China. Email: hjy219@126.com

Abstract

An understanding of the transport of silica nanoparticles (NPs) across the placental barrier is important in perinatal medicine. The cytotoxicity of silica NPs was investigated in this study. In uptake assays, we examined the size of NPs, as well as the effects of various inhibitors, on the internalization of silica NPs in BeWo b30 cells. The levels of PI3K, AKT, and GSK3 β were assessed after the cells were treated with silica NPs and/or the PI3K/AKT signaling pathway inhibitor LY294002. The integrity of the cell monolayer was assessed by culturing cells on Transwell inserts and measuring the transepithelial electrical resistance, assessing fluorescein sodium transport, and staining the tight junction protein zonula occludens-1. Silica NPs were spherical in shape, and concentrations <300 μ g/mL were not cytotoxic. The internalization of silica NPs with a diameter of 50 nm was greater than that of silica NPs with a diameter of 20 nm. CPZ showed the most pronounced inhibitory effects, with inhibition rates of 20-nm, 50-nm, and 100-nm silica NPs reaching 57.5%, 49.6%, and 46.9%, respectively, indicating that silica NPs were internalized through clathrin- and caveolae-mediated endocytosis. Furthermore, LY294002 affected the uptake of 50-nm silica NPs dose-dependently. The treatment of cells with silica NPs

also increased the levels of P-PI3K/PI3K, P-AKT/AKT, and P-GSK3 β /GSK3 β , while LY294002 inhibited the levels of these proteins, indicating that the internalization of silica NPs is regulated by the PI3K/AKT/GSK3 β signaling pathway. Taken collectively, these results provide new insights on the transplacental transport of NPs in perinatal medicine.

Keywords: silica nanoparticles; placental barrier; endocytosis; transport

Introduction

Over the past 20 years, nanotechnology has been used in the diagnosis and treatment of a variety of diseases [1]. Nanomedicine involves the use of nanoparticles (NPs), which can be used in magnetic resonance imaging, biosensor development, and drug delivery, as they facilitate targeted drug delivery and increase drug bioavailability [2,3]. Nanomedicine also has great potential in the treatment of maternal, fetal, and placental disorders. However, it is not known if NPs safe for use in pregnant women [4], and therefore, it is important to investigate the transplacental transport of NPs in this population.

NPs interact with components of the extracellular matrix and the plasma membrane and enter cells through endocytosis. Endocytosis is an important mechanism for the transport of NPs across the maternal–fetal barrier [5], and there are five different types of endocytosis, namely, caveolin-mediated endocytosis, phagocytosis, clathrin-mediated endocytosis, clathrin/caveolae-independent endocytosis, and micropinocytosis. Macromolecules, such as NPs, typically enter the placenta by pinocytosis/endocytosis and phagocytosis. BeWo b30 cells are human placental trophoblast cells that are often used to study transplacental transport mechanisms [6]. Li et al. investigated the transport of nine compounds and demonstrated a good correlation ($R^2 = 0.95$) between the transport indices of BeWo b30 cells and ex vivo models [7]. Albekairi et al. prepared biodegradable digoxin-loaded PEGylated poly (lactic-co-glycolic acid) NPs using a modified solvent displacement method and examined the permeability of these NPs across the BeWo b30 cell monolayer [8]. The results revealed that NPs exhibited sustained drug release kinetics, and nanoencapsulation could protect digoxin from P-glycoprotein (P-gp)-mediated efflux, thereby increasing maternal-to-fetal drug transfer. Kloet et al. analyzed the transport of NPs across the placental barrier using one positively-charged and two negatively-charged polystyrene NPs (PS-NPs) of similar size and revealed that the transport of PS-NPs across the BeWo b30 cell monolayer was not related to charge [9]. The specific transport mechanisms were also investigated using inhibitors of endocytosis or ABC transporters, and inhibitors of BCRP, P-gp, clathrin, and caveolin did not affect the transport of PS-NPs. Previously, we prepared fluorescein isothiocyanate (FITC) conjugated pullulan acetate (PA-FITC) NPs and investigated transplacental transport using the BeWo b30 cell line. We found that these NPs, which were nontoxic, could cross the blood–placental barrier, and BeWo b30 cells could internalize PA-FITC NPs through caveolae-mediated endocytosis and pinocytosis [10]. Although this research area has received significant attention, there are few studies on the transport of NPs across the placental barrier.

Silica NPs have been studied for their use as drug carriers or imaging agents. Properties, such as tunable size and shape, high surface area, and large pore volume, make mesoporous silica NPs particularly advantageous for controlled drug release [11]. However, there are few studies on the use of silica NPs in pregnancy. Yamashita et al. administered 70-nm, 300-nm, and 1000-nm silica NPs into pregnant mice and observed that only the 70-nm particles were distributed in the placenta [12]. However, due to structural and functional differences between the species [13], these findings may not be applicable to pregnant women. Poulsen et al. investigated the transport of 20-nm and 50-nm silica NPs across the BeWo b30 cell monolayer and the ex vivo perfused human placenta, revealed that the transport of silica NPs was limited with an apparent permeability of $1.54 \times 10^{-6} \pm 1.56 \times 10^{-6}$ cm/sec [14]. Furthermore, the percentage of 25-nm and 50-nm silica NPs reaching

the fetal perfusate after 6 h was limited to $4.2 \pm 4.9\%$ and $4.6 \pm 2.4\%$, respectively. The particles also accumulated both in vitro and in vivo, as confirmed by confocal microscopy. Therefore, silica NPs can cross the placental barrier, although the mechanism is unknown.

In this study, we examine the cytotoxicity of silica NPs using BeWo b30 cells. We investigate the possible mechanisms of transport and demonstrate the role of the PI3K/AKT/GSK3 β signaling pathway in the internalization of silica NPs. The integrity of the BeWo b30 cell monolayer is also evaluated in transepithelial electrical resistance and fluorescein sodium (Na-Flu) transport assays, as well as tight junction protein staining. After determining the nontoxic concentration of silica NPs, their transport mechanism was assessed using the in vitro model.

Experimental

Materials

Transwell (diameter, 12 mm; pore size, 3.0 μm) polycarbonate membrane inserts and 96-well opaque cell culture plates were purchased from Corning (Corning, NY, USA). The Millicell electrical resistance system was procured from Millipore (Bedford, MA, USA). The Cell Counting Kit-8 was purchased from Dojindo Laboratories (Kumamoto, Japan). Silica NPs of different sizes were procured from Suzhou Derivative Biotechnology (Suzhou, China). The BeWo b30 cell line was a gift from Professor Erik Rytting (University of Texas Medical Branch, Galveston, TX, USA). DMEM-F12 was purchased from Hyclone Corp. (Logan, UT, USA). Phenol red-free DMEM-F12 and fetal bovine serum (FBS) were purchased from Thermo Fisher Scientific (Waltham, MA, USA). The rabbit anti-human zonula occludens-1 (ZO-1) antibody and the goat anti-rabbit secondary antibody (conjugated to Alexa Fluor-488) were purchased from Thermo Fisher Scientific. Pharmacological inhibitors, Na-Flu salt, dimethyl sulfoxide, and 4',6-diamidino-2-phenylindole (DAPI) were procured from Sigma-Aldrich (St. Louis, MO, USA). Trypsin, Hank's balanced salt solution, and Triton X-100 were purchased from Beijing Solarbio Technology (Beijing, China). Phosphorylation-specific antibodies against GSK3- β (S9) and Akt (S473), as well as antibodies against GSK3- β , PI3K-p85, β -actin and AKT, were procured from Cell Signaling Technology (Danvers, MA, USA). The phosphorylation-specific PI3K-p85 (Tyr458) antibody was purchased from Abcam (Cambridge, UK).

Characterization of silica nanoparticles

Silica NPs with diameters of 20, 50, and 100 nm were labeled with rhodamine B, diluted with water (stock concentration, 25 mg/mL), and stored at 4°C. The size distribution of the silica NPs was measured by dynamic light scattering (DLS; Zetasizer 2000; Malvern Instruments Ltd., Malvern, UK). The average size was determined from SEM images by averaging the diameters of 100 particles. The morphology of the silica NPs was observed by transmission electron microscopy (TEM; EM100CXII; JEOL Ltd., Tokyo, Japan) and scanning electron microscopy (SEM; SUPRA 55VP; Carl Zeiss Microscopy GmbH, Jena, Germany). For TEM, a drop of the NP suspension was deposited on a copper grid and air-dried prior to observation. For SEM, a drop of the NP suspension was placed on a silicon wafer and air-dried. Subsequently, the samples were coated with gold for observation.

Cell culture

BeWo b30 cells were cultured in DMEM-F12, containing phenol red, 10% FBS, 4 mM L-glutamine, and 1% penicillin–streptomycin at 37°C in a humidified atmosphere with 5% CO₂. Upon reaching 75–80% confluence, the cells were subcultured using a 0.25% trypsin–EDTA solution.

CCK-8 cytotoxicity assay

BeWo b30 cells (1×10^4 cells/well) were seeded in 96-well plates and cultured for 24 h until confluence. The cells were treated with silica NPs at different concentrations (200, 300, 400, 600, 800 $\mu\text{g/ml}$) for 24 and 48 h. Untreated cells served as the negative control. Subsequently, the culture supernatant was removed, the cells were washed in PBS, CCK-8

reagent was added (10 μ L of CCK-8 in 100 μ L of medium), and the cells were incubated for 90 mins. The absorbance was measured at a wavelength of 450 nm with a microplate reader. The percentage of viable cells (CV%) was calculated as follows: $CV\% = \text{optical density (test)}/\text{optical density (control)} \times 100\%$.

Uptake of silica nanoparticles with different particle sizes and concentrations

BeWo b30 cells (1×10^4 cells/well) were seeded in 96-well opaque plates and cultured for 24 h, as indicated above. Subsequently, the culture supernatant was removed, silica NPs were added at different concentrations (300, 150, 75 μ g/mL), and the cells were incubated for 5 h. The cells were washed three times with ice-cold PBS, and cell lysis solution (100 μ L of 0.3% Triton X-100) was added for 1 h, after which the fluorescence intensity was measured, as indicated above. The cells cultured in the absence of NPs served as the blank control, and the cells cultured in the presence of NPs at the same concentration served as the negative control.

Effects of inhibitors on the uptake of silica nanoparticles

BeWo b30 cells (1×10^4 cells/well) were seeded in 96-well opaque plates, as indicated above. Subsequently, the culture supernatant was removed, silica NPs were added at a concentration of 300 μ g/mL, and the cells were incubated for 5 h. The cells were washed three times with ice-cold PBS, and cell lysis solution (100 μ L of 0.3% Triton X-100) was added for 1h, after which the fluorescence intensity was measured, as indicated above. The uptake of silica NPs was expressed as the optical density. The percent uptake was calculated as follows: $\text{uptake}\% = (\text{fluorescence intensity [test]}/\text{fluorescence intensity [control]}) \times 100\%$.

To examine the effects of inhibitors of endocytosis on the uptake of silica NPs, the cells were pre-incubated with CPZ at 7 μ g/mL to inhibit clathrin-mediated endocytosis, NY at 50 μ g/mL to inhibit caveolae-mediated endocytosis, Col at 10 μ g/mL to inhibit pinocytosis, and AMR at 50 μ M to inhibit micropinocytosis for 1 h as previously described [10]. Subsequently, the culture supernatant was removed, silica NPs were added at a concentration of 300 μ g/mL, and the cells were incubated for 5 h. The cells were washed, as indicated above. The cells cultured in the presence of silica NPs but in the absence of inhibitor served as the negative control. The uptake rate was expressed as 100%. The percent uptake was calculated as follows: $\text{uptake}\% = (\text{fluorescence intensity [test]}/\text{fluorescence intensity [control]}) \times 100\%$.

To examine the activation of the PI3K/AKT signaling pathway by silica NPs, the cells were pre-incubated with the PI3K/AKT inhibitor LY294002 at different concentrations (2.5, 5, 10 μ M) for 30 min. Subsequently, the culture supernatant was removed, silica NPs in medium containing the inhibitor at the indicated concentrations were added, and the cells were incubated for 2 h. The percent uptake was calculated, as indicated above.

Western blot assay

BeWo b30 cells were incubated with LY294002, as indicated above. Subsequently, the culture supernatant was removed, silica NPs in medium containing the inhibitor at the indicated concentrations were added, and the cells were incubated for 2 h. The cells cultured in the absence of the inhibitor served as the negative control, whereas the cells cultured in the presence of silica NPs but in the absence of the inhibitor served as the positive control. The cells were terminated by cell lysis buffer (50 μ L of 0.3% Triton X-100), containing phosphatase inhibitor cocktail (1:100) and phenylmethylsulfonyl fluoride (1:100). The cells were frozen and thawed three times, and the samples were centrifuged (4 $^{\circ}$ C, 12000 rpm, 5 min). The protein concentration was measured by the BCA method. Subsequently, equivalent amounts of protein were separated by SDS-PAGE. The proteins were transferred to PVDF membranes, and the membranes were blocked with 5% bovine serum albumin for 2 h and incubated with primary antibodies for 18 h at 4 $^{\circ}$ C. The membranes were washed with TBST three times, 10 min each time, and incubated with secondary antibodies for 70 min at room temperature. The target proteins were visualized with the Tanon 5200 Automatic Chemiluminescence Imaging Analysis System (Tanon Technology Co., LTD, Shanghai, China), and the relative gray-scale values were analyzed with Image Studio Software.

Establishment of in vitro placental model

Upon reaching 80–85% confluence, BeWo b30 cells (1×10^5 cells/insert) were seeded in Transwell inserts and cultured for 7 days, as indicated above. Transepithelial electrical resistance (TEER) was measured each day as previously described [15]. On day 6, the transport of Na-Flu was assessed, and the tight junction protein ZO-1 was stained.

Transport of silica nanoparticles

This experiment required the use of phenol red-free DMEM-F12. BeWo cells (1×10^5 cells/insert) were seeded on Transwell inserts and cultured for 24 h until confluence. Subsequently, the culture supernatant was removed. At time 0, 0.5 mL of 50-nm silica NPs was added to the upper chamber at a concentration of 300 $\mu\text{g}/\text{mL}$ and 1.5 mL of media was added to the lower chamber. After 2, 4, 6, 8, 12, 16, 20 and 24 h, a 50- μL aliquot of the medium was collected from the lower chamber, which was transferred to a 96-well opaque plate, and 50 μL of the medium was added to the lower chamber. After the last collection of the medium, the TEER was measured, and the cells were washed, as indicated above. The membranes were excised, fixed in 2% paraformaldehyde for 40 min, permeabilized in 0.3% Triton X-100 for 20 min at room temperature, and blocked in 3% BSA in PBS for 1 h at room temperature. The cells were incubated with the rabbit anti-human ZO-1 antibody (diluted 1:100 in 2% bovine serum albumin in PBS) for 18 h at 4°C, followed by the secondary antibody (diluted 1:1000 in PBS) for 1 h at room temperature in the dark. The nuclei were stained with DAPI, and the membranes were mounted on glass slides. The cells were observed under a confocal laser scanning microscope (A1R+; Nikon Ltd., Tokyo, Japan), and the images were processed with NIS-Elements Viewer 5.21 Software.

To examine the effects of the inhibitors on the uptake of silica NPs, the cells were cultured on Transwell inserts and pre-incubated with silica NPs. The concentrations of the inhibitors were the same as those of previous experiments, and the percent uptake was calculated, as indicated above.

Statistical analysis

Data were presented as mean \pm SD. Statistical significance was determined by one-way analysis of variance, and P-values <0.05 were considered significant.

Results and Discussion

Characterization of silica NPs

The silica NPs were uniform in size and spherical in shape (Figure 1 and Figure 2). The diameters of the silica NPs were determined by SEM to be 36.0 ± 4.8 nm, 54.0 ± 6.0 nm, and 133.9 ± 19.4 nm ($n = 100$), and the distribution of the sizes was assessed by DLS to be narrow. The ζ potentials were -25.56 ± 1.354 mV, -37.36 ± 1.790 , and -33.63 ± 2.661 ($n = 3$), indicating good stability in aqueous solution.

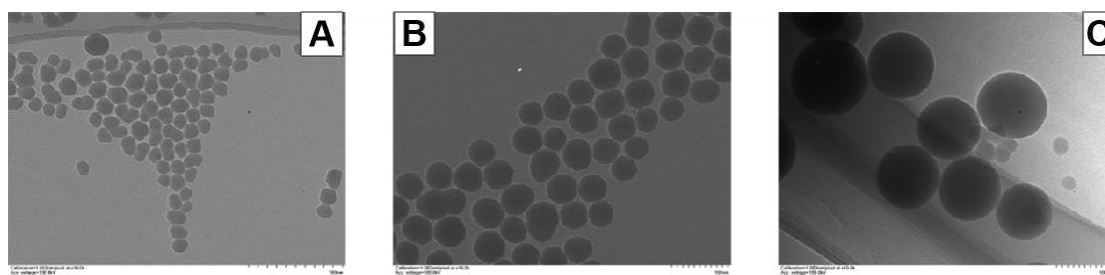


Figure 1 TEM images of silica NPs. (A) 20-nm silica NPs, (B) 50-nm silica NPs, and (C) 100-nm silica NPs.

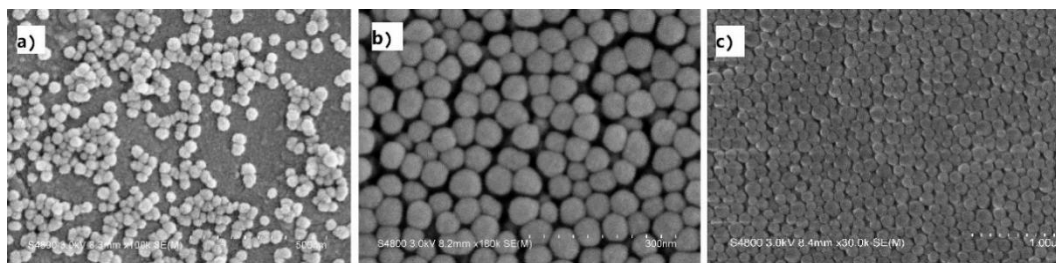


Figure 2 SEM images of silica NPs. (A) 20-nm silica NPs, (B) 50-nm silica NPs, and (C) 100-nm silica NPs.

3.2 CCK-8 cytotoxicity assay

Silica NPs at concentrations $<400 \mu\text{g/mL}$ were not cytotoxic. There were no apparent toxic effects of silica NPs of different sizes on BeWo b30 cells, consistent with those of Carreira et al [16]. However, 50-nm and 100-nm silica NPs at concentrations $>400 \mu\text{g/mL}$ were cytotoxic, and 20-nm silica NPs at a concentration of $800 \mu\text{g/mL}$ were also cytotoxic (Figure 3). Therefore, uptake and transport assays were performed at a concentration of $300 \mu\text{g/mL}$.

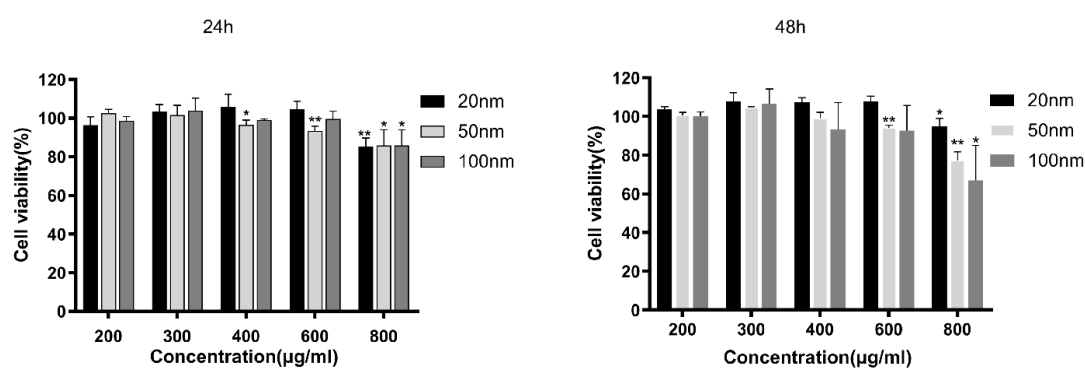


Figure 3 Viability of BeWo b30 cells exposed to silica NPs for 24 and 48 h. Each value represents the mean \pm SD (n = 5).

3.3 Uptake of silica nanoparticles of different sizes and concentrations

The uptake of silica NPs increased as the concentration of silica NPs increased (Figure 4), indicating that the uptake by BeWo b30 cells was not saturated at $300 \mu\text{g/mL}$. At concentrations of 75 and $150 \mu\text{g/mL}$, the uptake of 50-nm silica NPs was significantly greater than that of 20-nm and 100-nm silica NPs. The result was same with Nam et al.[17], NP internalization increases with NP size, and the uptake rate was highest for 45–50-nm NPs, whereas the exocytic rate was fastest for smaller NPs. At a concentration of $300 \mu\text{g/mL}$, the uptake of 100-nm silica NPs was the greatest, indicating that the internalization of silica NPs was related to size.

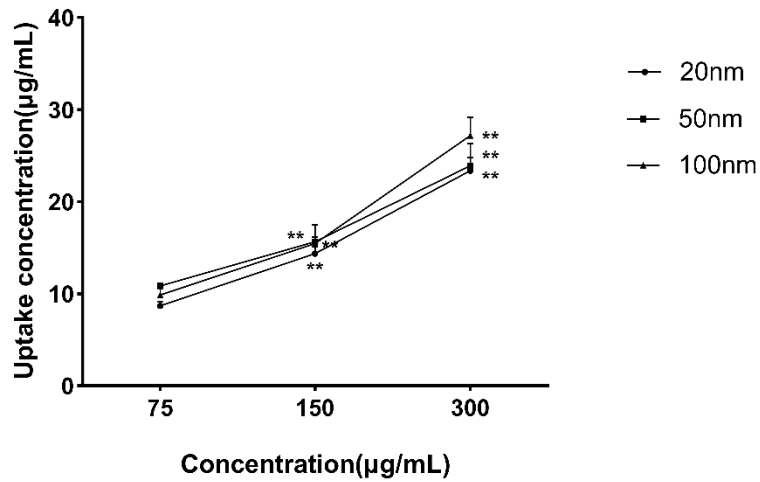


Figure 4 Dose-dependent uptake of silica NPs by BeWo b30 cells. The cells were incubated with 20-nm, 50-nm, and 100-nm silica NPs (300 µg/mL) for 5 h, and the uptake was quantified by fluorometry. Data are represented as mean ±SD of five determinations. **, P < 0.01 compared to a concentration of 75 µg/mL.

3.4 Monolayer confirmation

BeWo b30 cells can establish a monolayer, and they are often used as a model of the human placental barrier for studying transplacental transport [6]. We evaluated the formation of the cell monolayer from days 1 to 7 using TEER and Na-Flu transport assays and observed that tight junctions were established during this time. TEER values higher than 60 Ω cm² were considered acceptable for performing subsequent transport experiments [18]. On day 5, the results of TEER and Na-Flu assays confirmed the formation of the BeWo b30 cell monolayer (Figure 5). On day 6, the results of ZO-1 staining further confirmed the formation of the cell monolayer, the nuclei were visualized with DAPI (Figure 6). The research progress consistent with the results of previous studies [8,10,15].

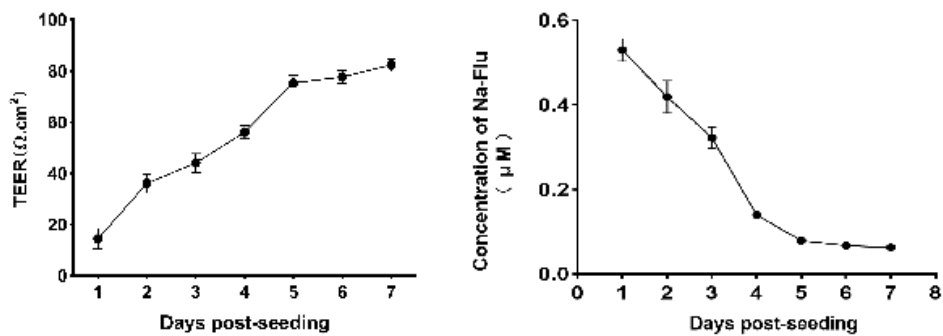


Figure 5 Formation of BeWo b30 cell monolayer. (A) Results of TEER assay, (B) Results of Na-Flu transport assay. Data are represented as mean ± SD of five determinations.

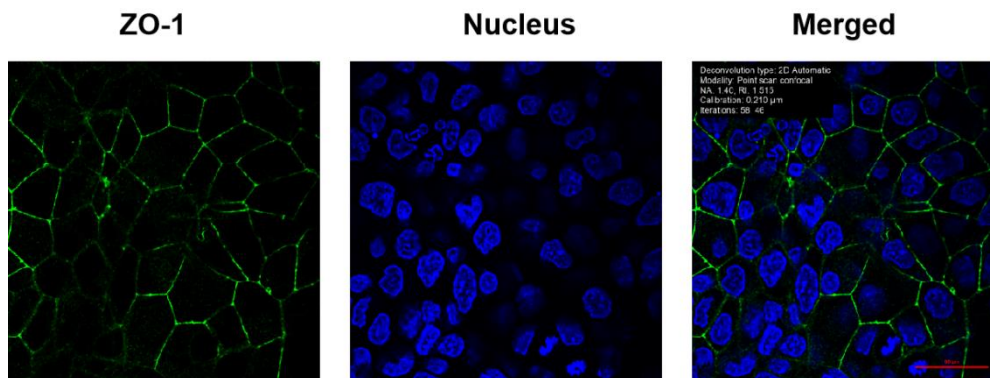


Figure 6 Confocal images of BeWo b30 cells fluorescently stained for ZO-1. The cells were cultured on Transwell units and stained with an antibody against ZO-1 (green). The cell nuclei were stained with DAPI (blue).

3.5 Transport of silica nanoparticles

The results of the transport of silica NPs across the BeWo b30 cell monolayer are shown in Figure 7. The transport rate was fast from 0 to 12 h and slow after 12 h. The concentration increased from 0 $\mu\text{g/mL}$ to 60.7 $\mu\text{g/mL}$ and 7.6 $\mu\text{g/mL}$, respectively, indicating that silica NPs were capable of transplacental transport.

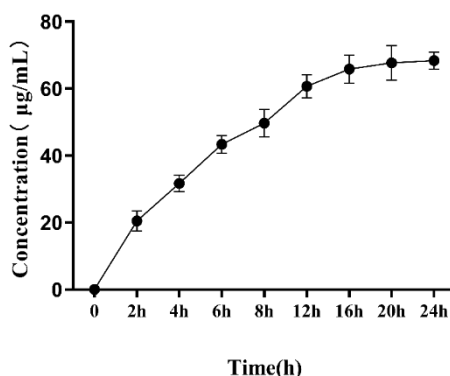


Figure 7 Transport of 50-nm silica NPs across the BeWo b30 cell monolayer. The cells were incubated with 50-nm silica NPs at a concentration of 300 $\mu\text{g/mL}$ for 24 h, and the concentrations of silica NPs in the lower chamber were quantified at different time points by fluorometry. Data are represented as mean \pm SD of three determinations.

3.6 Endocytic mechanism of silica NPs

The cellular uptake of NPs was suppressed by inhibitors of endocytosis. The internalization of 20-nm, 50-nm, and 100-nm silica NPs was reduced significantly after treating cells with inhibitors of endocytosis ($P < 0.05$ or $P < 0.01$) (Figure 8). CPZ showed the most pronounced inhibitory effect, with inhibition rates of 20-nm, 50-nm, and 100-nm silica NPs reaching 57.5%, 49.6%, and 46.9%, respectively. NY also showed a significant inhibitory effect, with inhibition rates of 20-nm, 50-nm, and 100-nm silica NPs reaching 43.2%, 34.9%, and 39.4%, respectively. By confocal microscopy, silica NPs were observed in the cytoplasm of BeWo b30 cells (Figure 9). The number of silica NPs was decreased in CPZ- and NY-treated cells compared with Col- and AMR-treated cells, indicating that the internalization of silica NPs involves clathrin- and caveolin-mediated endocytosis. CPZ, a selective inhibitor of clathrin-mediated endocytosis, showed the most pronounced effect, followed by the caveolin-mediated endocytosis inhibitor, NY, and these findings were confirmed by confocal microscopy. These results indicate that clathrin- and caveolae-mediated endocytosis are involved in the internalization of silica NPs, consistent with a previous study that revealed clathrin-mediated endocytosis of 310-nm silica

NPs in HUVECs [19]. Another study in fibroblasts demonstrated that 500-nm silica NPs were internalized by clathrin-mediated endocytosis and macropinocytosis but 80-nm NPs were internalized by clathrin-mediated endocytosis, micropinocytosis, and caveolae-mediated endocytosis [20]. Taken together, clathrin- and caveolin-dependent mechanisms play roles in the uptake of silica NPs of different sizes.

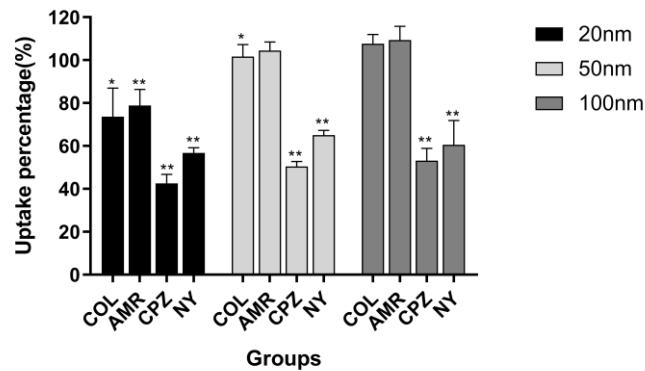


Figure 8 Effects of inhibitors of endocytosis on the internalization of silica NPs. BeWo b30 cells were pre-treated with different inhibitors of endocytosis for 1 h and then treated with silica NPs at a concentration of 300 $\mu\text{g/mL}$. The percent uptake was quantified by fluorometry. Data are presented as mean \pm SD of five determinations. *, $P < 0.05$; **, $P < 0.01$ compared to respective controls. AMR, amiloride; Col, colchicine; CPZ, chlorpromazine; NY, nystatin.

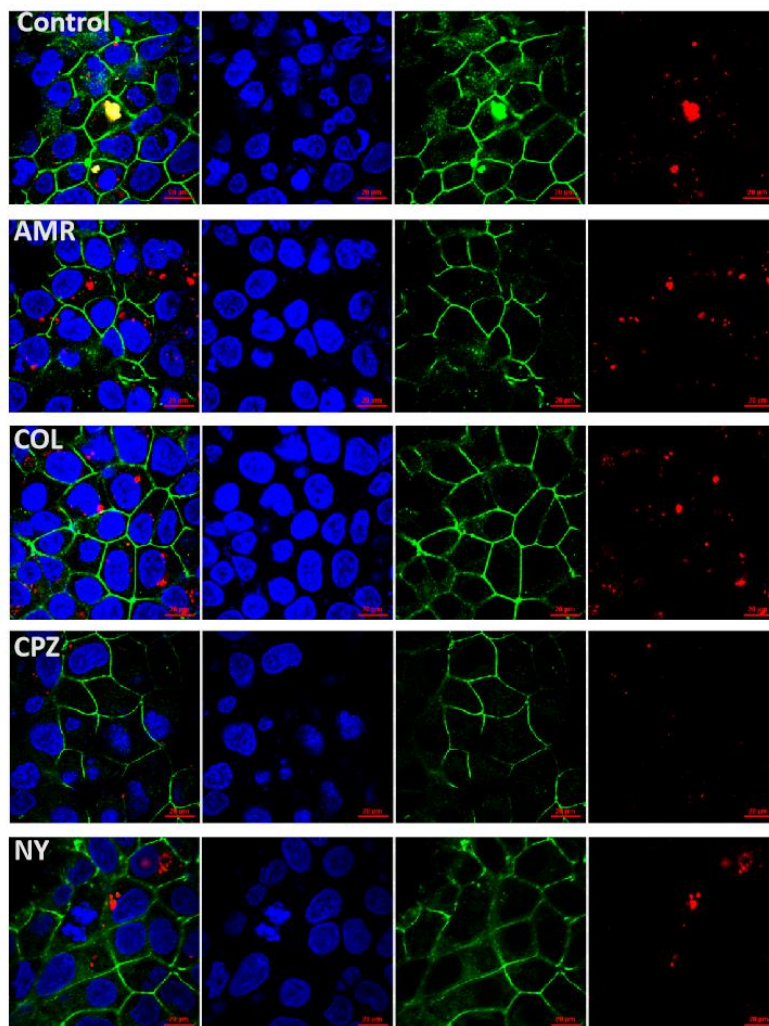


Figure 9 Confocal images of BeWo b30 cells treated with different inhibitors of endocytosis. The cells were cultured on

Transwell units, treated with amiloride (AMR), colchicine (Col), chlorpromazine (CPZ) or nystatin (NY) as indicated, and stained with an antibody against ZO-1 (green). The cell nuclei were stained with DAPI (blue). Silica NPs (diameter, 50-nm; red) are shown in the cytoplasm.

3.7 PI3K/AKT/GSK3 β signaling pathway in the endocytosis of silica nanoparticles

To investigate the dose-dependent effects of the PI3K/AKT inhibitor on the uptake of 50-nm silica NPs, BeWo b30 cells were pre-treated with LY294002 at concentrations of 2.5, 5, and 10 μ M for 30 min. All three doses of the inhibitor affected the internalization of silica NPs dose-dependently, with inhibitory rates of 31.05%, 36.14%, and 43.53%, respectively ($P < 0.01$) (Figure 10). The levels of PI3K, AKT, and GSK3 β were evaluated by western blot (Figure 11). When the cells were treated with silica NPs, the levels of P-PI3K/PI3K, P-AKT/AKT, and P-GSK3 β /GSK3 β increased compared with control cells. However, when the cells were pre-treated with LY294002 and then treated with silica NPs, the levels of these proteins decreased ($P < 0.05$ or $P < 0.01$). By confocal microscopy, the number of silica NPs in the cytoplasm of cells treated with LY294002 decreased compared with control cells, especially at concentrations of 5 and 10 μ M (Figure 12). These findings were consistent with those of uptake assays, and they indicate that the PI3K/AKT/GSK3 β signaling pathway plays important roles in internalization of the silica NPs, consistent with the results of Akira et al., who reported that treatment of bovine aortic endothelial cells with 70-nm silica NPs increased the p-AKT/total AKT level compared with the control, whereas wortmannin, a selective PI3K inhibitor, decreased its level [21].

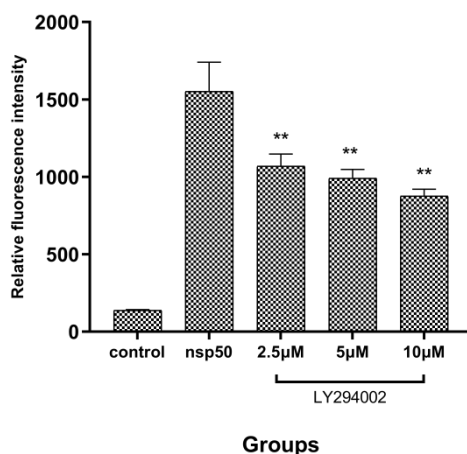


Figure 10 Effects of the PI3K/AKT inhibitor on the internalization of silica NPs. BeWo b30 cells were pre-treated with LY294002 for 30 min and then treated with 50-nm silica NPs at a concentration of 300 μ g/mL. Internalization was quantified by fluorometry. Data are represented as mean \pm SD of five determinations. **, $P < 0.01$ compared to 50-nm silica NPs alone.

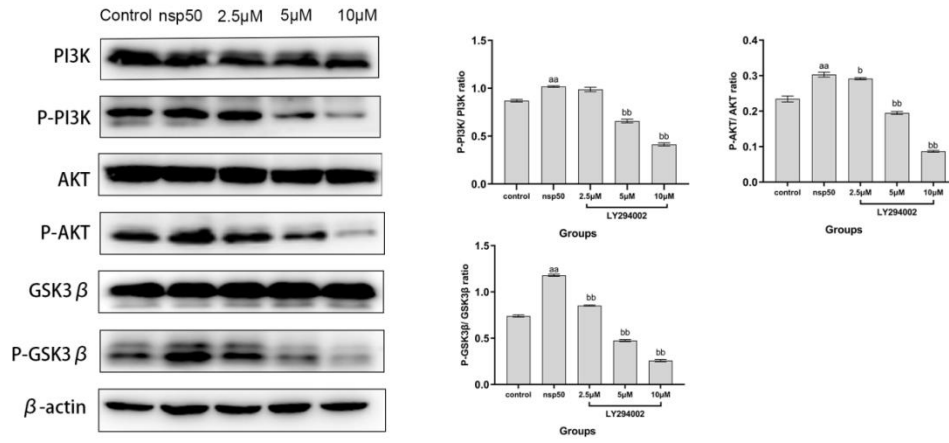


Figure 11 Levels of PI3K, P-PI3K, AKT, P-AKT, GSK3β, and P-GSK3β following treatment. BeWo b30 cells were pre-treated with LY294002 at different concentrations (2.5, 5, 10 μM) for 30 min and then treated with 50-nm silica NPs at a concentration of 300 μg/mL. Protein levels were quantified by western blotting. Data are represented as mean ± SD of three determinations. ^{aa}, P < 0.01 compared to respective controls; ^b, P < 0.05; ^{bb}, P < 0.01 compared to 50-nm silica NPs alone.

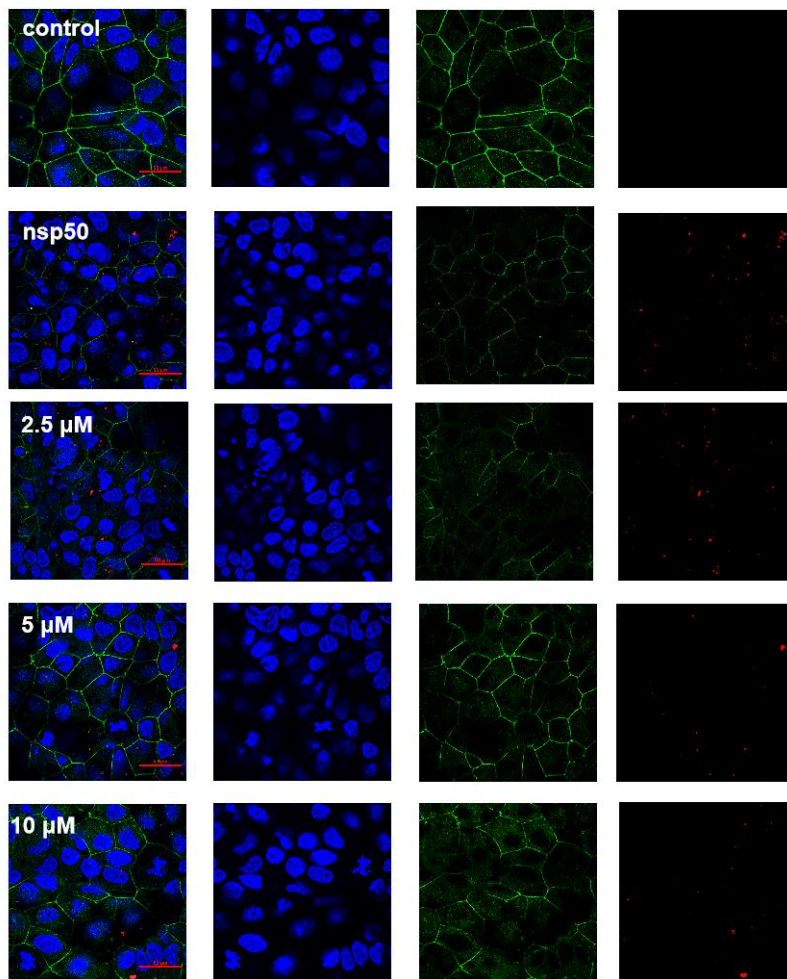


Figure 12 Confocal images of BeWo b30 cells treated with the PI3K/AKT inhibitor. BeWo b30 cells were treated with LY294002 at different concentrations (2.5, 5, 10 μM). The tight junction protein ZO-1 was stained, and the cell nuclei were

stained with DAPI. Silica NPs (diameter, 50 nm; red) are shown in the cytoplasm.

Conclusion

Taken collectively, silica NPs can cross the BeWo b30 cell monolayer, and they are internalized by clathrin- and caveolin-mediated endocytosis, which is regulated by the PI3K/AKT/GSK3 β signaling pathway. The internalization of silica NPs by BeWo b30 cells was affected by the size of NPs. Our findings indicate that this approach of endocytic inhibition can reduce the fetal toxicity of nanomedicines and promote their application in perinatal medicine.

Acknowledgments

All the authors thank Professor Erik Rytting (University of Texas Medical Branch) for donating the choriocarcinoma cell line BeWo b30. This work was financially supported by Capital Medical University (No. PYZ2018126, PYZ19056)

Conflict of interest

The authors declare that they have no conflict of interests.

ORCID® iDs

Hongbo Tang - <https://orcid.org/0000-0003-3048-8353>

References

1. Adepu, S.; Ramakrishna, S. Controlled Drug Delivery Systems: Current Status and Future Directions. *Molecules*. 2021, 26(19), 5905. doi:10.3390/molecules26195905
2. Farjadian, F.; Ghasemi, A.; Gohari, O.; Roojintan, A. ; Karimi, M. ; & Hamblin, M. R. Nanopharmaceuticals and nanomedicines currently on the market: challenges and opportunities. *Nanomedicine*. 2019, 14(1), 93–126. doi:10.2217/nmm-2018-0120
3. Sato, Y.; Nakamura, T.; Yamada, Y.; Harashima, H. The nanomedicine rush: New strategies for unmet medical needs based on innovative nano DDS. *J Control Release*. 2021,330, 305–316. doi:10.1016/j.jconrel.2020.12.032
4. Aengenheister, L. ; Favaro, R. R. ; Morales-Prieto, D. M. ; Furer, L. A. ; Gruber, M. ; Wadsack, C. ; Markert, U. R. ; Buerki-Thurnherr, T. Research on nanoparticles in human perfused placenta: State of the art and perspectives. *Placenta*. 2021,104, 199–207. doi:10.1016/j.placenta.2020.12.014
5. Cooke, L. ; Tumbarello, D. A. ; Harvey, N. C. ; Sethi, J. K. ; Lewis, R. M. ; Cleal, J. K. Endocytosis in the placenta: An undervalued mediator of placental transfer. *Placenta*. 2021,113, 67–73. doi:10.1016/j.placenta.2021.04.014
6. Nikulin, S. V. ; Knyazev, E. N. ; Gerasimenko, T. N. ; Shilin, S. A. ; Gazizov, I. N. ; Zakharova, G. S. ; Poloznikov, A. A. ; Sakharov, D. A. *Mol Biol*. 2019,53(3), 467–475. doi:10.1134/S0026898419030133
7. Li, H. ; van Ravenzwaay, B. ; Rietjens, I. M. ; Louisse, J. Assessment of an in vitro transport model using BeWo b30 cells to predict placental transfer of compounds. *Arch Toxicol*. 2013,87(9), 1661–1669. doi:10.1007/s00204-013-1074-9
8. Albekairi, N. A. ; Al-Enazy, S. ; Ali, S. ; Rytting, E. Transport of digoxin-loaded polymeric nanoparticles across BeWo cells, an in vitro model of human placental trophoblast. *Ther Deliv*. 2015,6(12), 1325–1334. doi:10.4155/tde.15.79
9. Kloet, S. K. ; Walczak, A. P. ; Louisse, J. ; van den Berg, H. H. ; Bouwmeester, H. ; Tromp, P. ; Fokkink, R. G. ;

- Rietjens, I. M. Translocation of positively and negatively charged polystyrene nanoparticles in an in vitro placental model. *Toxicol In Vitro*. 2015,29(7), 1701–1710. doi:10.1016/j.tiv.2015.07.003
10. Tang, H. ; Jiang, Z. ; He, H. ; Li, X. ; Hu, H. ; Zhang, N. ; Dai, Y. ; Zhou, Z. Uptake and transport of pullulan acetate nanoparticles in the BeWo b30 placental barrier cell model. *Int J Nanomedicine*. 2018,13, 4073–4082. doi:10.2147/IJN.S161319
 11. Yang, Y. ; Zhang, M. ; Song, H. ; Yu, C. Silica-Based Nanoparticles for Biomedical Applications: From Nanocarriers to Biomodulators. *Acc Chem Res*. 2020,53(8), 1545–1556. doi:10.1021/acs.accounts.0c00280
 12. Yamashita, K. ; Yoshioka, Y. ; Higashisaka, K. ; Mimura, K. ; Morishita, Y. ; Nozaki, M. ; Yoshida, T. ; Ogura, T. ; Nabeshi, H. ; Nagano, K. ; Abe, Y. ; Kamada, H. ; Monobe, Y. ; Imazawa, T. ; Aoshima, H. ; Shishido, K. ; Kawai, Y. ; Mayumi, T. ; Tsunoda, S. ; Itoh, N. ; Tsutsumi, Y. Silica and titanium dioxide nanoparticles cause pregnancy complications in mice. *Nat Nanotechnol*. 2011,6(5), 321–328. doi:10.1038/nnano.2011.41
 13. Carter A. M. Animal models of human pregnancy and placentation: alternatives to the mouse. *Reproduction*. 2020,160(6), R129–R143. doi:10.1530/REP-20-0354
 14. Poulsen, M. S. ; Mose, T. ; Maroun, L. L. ; Mathiesen, L. ; Knudsen, L. E. ; Rytting, E. Kinetics of silica nanoparticles in the human placenta. *Nanotoxicology*. 2015,9 Suppl 1(0 1), 79–86. doi:10.3109/17435390.2013.812259
 15. Cartwright, L. ; Poulsen, M. S. ; Nielsen, H. M. ; Pojana, G. ; Knudsen, L. E. ; Saunders, M. ; Rytting, E. In vitro placental model optimization for nanoparticle transport studies. *Int J Nanomedicine*. 2012,7, 497–510. doi:10.2147/IJN.S26601
 16. Correia Carreira, S. ; Walker, L. ; Paul, K. ; Saunders, M. The toxicity, transport and uptake of nanoparticles in the in vitro BeWo b30 placental cell barrier model used within NanoTEST. *Nanotoxicology*. 2015,9 Suppl 1, 66–78. doi:10.3109/17435390.2013.833317
 17. Nam, J. ; Won, N. ; Bang, J. ; Jin, H. ; Park, J. ; Jung, S. ; Jung, S. ; Park, Y. ; Kim, S. Surface engineering of inorganic nanoparticles for imaging and therapy. *Adv Drug Deliv Rev*. 2013,65(5), 622–648. doi:10.1016/j.addr.2012.08.015
 18. Mørck, T. J. ; Sorda, G. ; Bechi, N. ; Rasmussen, B. S. ; Nielsen, J. B. ; Ietta, F. ; Rytting, E. ; Mathiesen, L. ; Paulesu, L. ; Knudsen, L. E. Placental transport and in vitro effects of Bisphenol A. *Reprod Toxicol*. 2010,30(1), 131–137. doi:10.1016/j.reprotox.2010.02.007
 19. Blechinger, J. ; Bauer, A. T. ; Torrano, A. A. ; Gorzelanny, C. ; Bräuchle, C. ; Schneider, S. W. Uptake kinetics and nanotoxicity of silica nanoparticles are cell type dependent. *Small*. 2013, 9(23), 3970–3906. doi:10.1002/sml.201301004
 20. Zhang, Y. ; Hu, L. ; Yu, D. ; Gao, C. Influence of silica particle internalization on adhesion and migration of human dermal fibroblasts. *Biomaterials*. 2010, 31(32), 8465–8474. doi:10.1016/j.biomaterials.2010.07.060

21. Onodera, A. ; Yayama, K. ; Tanaka, A. ; Morosawa, H. ; Furuta, T. ; Takeda, N. ; Kakiguchi, K. ; Yonemura, S. ; Yanagihara, I. ; Tsutsumi, Y. ; Kawai, Y. Amorphous nanosilica particles evoke vascular relaxation through PI3K/Akt/eNOS signaling. *Fundam Clin Pharmacol.* 2016, 30(5), 419–428. doi: 10.1111/fcp.12206